

## Original Article



## OPEN ACCESS

**Received:** Jan 8, 2023  
**Revised:** Mar 27, 2023  
**Accepted:** Apr 15, 2023  
**Published online:** May 8, 2023

### \*Correspondence to

Young-Min Hyun

Department of Anatomy, Brain Korea 21 PLUS Project for Medical Science, Yonsei University College of Medicine, 50 Yonsei-ro, Seodaemun-gu, Seoul 03722, Korea.  
Email: ymhyun@yuhs.ac

Copyright © 2023. The Korean Association of Immunologists

This is an Open Access article distributed under the terms of the Creative Commons Attribution Non-Commercial License (<https://creativecommons.org/licenses/by-nc/4.0/>) which permits unrestricted non-commercial use, distribution, and reproduction in any medium, provided the original work is properly cited.

### ORCID iDs

Da Jeong Byun   
<https://orcid.org/0000-0002-5104-3057>  
Jaeho Lee   
<https://orcid.org/0000-0001-7946-0699>  
Je-Wook Yu   
<https://orcid.org/0000-0001-5943-4071>  
Young-Min Hyun   
<https://orcid.org/0000-0002-0567-2039>

### Conflict of Interest

The authors declare no potential conflicts of interest.

### Abbreviations

BBB, blood-brain barrier; CItH3, citrullinated histone H3; DAMP, damage-associated

# NLRP3 Exacerbate NETosis-Associated Neuroinflammation in an LPS-Induced Inflamed Brain

Da Jeong Byun <sup>1</sup>, Jaeho Lee <sup>1</sup>, Je-Wook Yu <sup>2</sup>, Young-Min Hyun <sup>1,\*</sup>

<sup>1</sup>Department of Anatomy, Brain Korea 21 PLUS Project for Medical Science, Yonsei University College of Medicine, Seoul 03722, Korea

<sup>2</sup>Department of Microbiology and Immunology, Institute for Immunology and Immunological Diseases, Brain Korea 21 Project for Medical Science, Yonsei University College of Medicine, Seoul 03722, Korea

## ABSTRACT

Neutrophil extracellular traps (NETs) exert a novel function of trapping pathogens. Released NETs can accumulate in inflamed tissues, be recognized by other immune cells for clearance, and lead to tissue toxicity. Therefore, the deleterious effect of NET is an etiological factor, causing several diseases directly or indirectly. NLR family pyrin domain containing 3 (NLRP3) in neutrophils is pivotal in signaling the innate immune response and is associated with several NET-related diseases. Despite these observations, the role of NLRP3 in NET formation in neuroinflammation remains elusive. Therefore, we aimed to explore NET formation promoted by NLRP3 in an LPS-induced inflamed brain. Wild-type and NLRP3 knockout mice were used to investigate the role of NLRP3 in NET formation. Brain inflammation was systemically induced by administering LPS. In such an environment, the NET formation was evaluated based on the expression of its characteristic indicators. DNA leakage and NET formation were analyzed in both mice through Western blot, flow cytometry, and *in vitro* live cell imaging as well as two-photon imaging. Our data revealed that NLRP3 promotes DNA leakage and facilitates NET formation accompanied by neutrophil death. Moreover, NLRP3 is not involved in neutrophil infiltration but is predisposed to boost NET formation, which is accompanied by neutrophil death in the LPS-induced inflamed brain. Furthermore, either NLRP3 deficiency or neutrophil depletion diminished pro-inflammatory cytokine, IL-1 $\beta$ , and alleviated blood-brain barrier damage. Overall, the results suggest that NLRP3 exacerbates NETosis *in vitro* and in the inflamed brain, aggravating neuroinflammation. These findings provide a clue that NLRP3 would be a potential therapeutic target to alleviate neuroinflammation.

**Keywords:** Neutrophil extracellular traps; NLR family pyrin domain-containing 3 protein; Brain; Inflammation; Intravital microscopy

## INTRODUCTION

Among the innate immune cells, neutrophils have been shown to react the fastest to pathogens, rapidly accumulating in sites of invasion, stimulation, and inflammation. The neutrophil performs highly versatile immunological functions on unwanted substances and pathogens through diverse mechanisms, with releasing extracellular traps, known as the

molecular pattern; HBSS, Hanks' balanced salt solution; i.v., intravenous; IHC, immunohistochemistry; KO, knockout; MPO, myeloperoxidase; NE, neutrophil elastase; NET, neutrophil extracellular trap; NLRP3, NLR family pyrin domain containing 3; ns, not significant; PAMP, pathogen-associated molecular pattern; PI, propodeum iodide; SIP, stock isotonic percoll; WGA, wheat germ agglutinin; WT, wild-type; ZO-1, Zonula Occludens-1.

#### Author Contributions

Conceptualization: Yu JW, Hyun YM; Data curation: Byun DJ, Lee J; Funding acquisition: Hyun YM; Validation: Byun DJ; Writing - original draft: Byun DJ, Hyun YM; Writing - review & editing: Hyun YM.

neutrophil extracellular traps (NETs) as a notable example (1-3). However, it has been recently reported that NETs can cause several diseases, such as sepsis and thrombosis, either directly or indirectly by themselves, activating other immune cells and increasing pro-inflammatory cytokines (4-6). NETs have been noted as an etiological factor particularly in brain diseases, such as multiple sclerosis, stroke, Alzheimer's disease, and traumatic brain injury (7-9). Although its association with these diseases has been verified, the relationship between NET formation and a relatable molecule involved in its neuropathology remains largely unknown. NETs are a meshwork of tangled neutrophil components with an extracellular DNA backbone. In response to stimuli, granular proteins, such as myeloperoxidase (10), neutrophil elastase (NE) (9), and protein arginine deiminase 4 (11), are activated. Chromatin is decondensed, and histone complex is citrullinated as an especially requisite characteristic of NET formation (12-14). Following this order of cellular processes, the endomembrane is fragmented, and the granule protein is secreted outside, accompanied by plasma membrane rupture (15,16). Emitted NETs have sticky properties that result in their accumulation in the inflamed tissue, further triggering other immune cells and causing tissue toxicity (6,17,18).

In this study, we explored the role of the NLR family pyrin domain containing 3 (NLRP3) inflammasome in NET formation. Inflammasomes are multi-protein complexes that play a pivotal role in signaling innate immune response after stimulation and are found in innate immune cells, including neutrophils (19-21). As a cytosolic complex, NLRP3 inflammasome is activated by various stimuli, such as pathogen-associated molecular patterns (PAMPs) and damage-associated molecular patterns (DAMPs). Upon activation, the NLRP3 inflammasome promotes the maturation of pro-inflammatory cytokines, such as IL-1 $\beta$  and IL-18, leading to a robust inflammatory response (22,23). Among the inflammasomes, the role of NLRP3 in several NET-related diseases has been noted (10,24). For example, a gain-of-function mutation in NLRP3 provokes Familial Mediterranean fever associated with NET formation, while the Muckle-Wells syndrome, which is implicated in excessive neutrophil granule exocytosis, is caused by an activation mutation in NLRP3 (25-27). Regardless of these findings, the role of NLRP3 in NET formation in the inflamed brain caused by the septic condition is still poorly understood and is therefore focused upon in this study.

Neuroinflammation is defined as the response of brain cells to infections and other causes of cell death, implicating the initiation of the immune system activity. Such inflammatory response in the brain is characterized by the destruction of the blood-brain barrier (BBB), infiltration, and activation of neuroglia and immune cells, during the onset of various neurological diseases, such as Alzheimer's disease, Parkinson's disease, and multiple sclerosis (28). Previous studies have verified the capability of systemic administrating LPS to cause the infiltration of innate immune cells into the brain, accompanied by the BBB breakdown (29-31). Furthermore, LPS can prime NLRP3 activation (22). Accordingly, we used the LPS-induced neuroinflammatory model to address the role of NLRP3 in NET formation in neurological diseases. To this end, we observed NET formation in control as well as NLRP3 knockout (KO) mice following the induction of neuroinflammation via LPS injection. We believe that our findings emphasize NLRP3 as a potential therapeutic target in several neurological diseases.

## MATERIALS AND METHODS

### Animal and LPS-induced neuroinflammatory model

The septic neuroinflammation mouse model for optimal NET generation was induced by an intravenous injection of 2.5 mg/kg *Escherichia coli*-derived LPS (O111:B4, Sigma-Aldrich, St. Louis, MO, USA) for 24 h. C57BL/6 mice (Orient Bio, Seongnam, Korea) and NLRP3 KO (Jackson Laboratory, Farmington, CT, USA) were maintained in a specific pathogen-free environment at Avison Biomedical Research Center at the Yonsei University College of Medicine. All animal experiments were approved by the Institutional Animal Care and Use Committee of the Yonsei University College of Medicine (IACUC No. 2019–0097).

### Neutrophil isolation

Wild-type (WT) and NLRP3 KO mice were sacrificed in a CO<sub>2</sub> chamber, and bone marrow cells were obtained from the femur and tibia. Obtained bone marrow cells were incubated with 2 ml of ammonium-chloride-potassium lysis buffer at 25°C for 5 min. Incubated cells were washed in PBS, and cell pellets were suspended in a buffer containing 2 mM EDTA and 2% FBS in PBS. Neutrophils were isolated through negative selection with a neutrophil isolation kit (Miltenyi Biotec, Bergisch Gladbach, Germany), following the manufacturer's description (32).

### Plasma membrane breakdown live cell imaging

Plasma membrane damage was compared in neutrophils isolated from WT and NLRP3 KO mice. Confocal dishes were coated with 10 µg/ml fibronectin (Thermo Fisher Scientific, Waltham, MA, USA) in 5% CO<sub>2</sub>, 37°C for 1 h. Isolated neutrophils (2×10<sup>5</sup>) from WT and NLRP3 KO bone marrow were seeded onto the surface of coated dishes and incubated for 30 min. To stimulate neutrophils, 1 µg/ml of *E. coli*-derived LPS was used, with PBS as the control; 5 µM of SYTOX-Orange impermeable nucleic acid stain (Thermo Fisher Scientific) was used to detect the plasma membrane breakdown (33–35). The cells incubated with SYTOX and LPS were diluted in RPMI 1640 media containing 10% FBS and 1% prostate-specific Ag. After 1 h of incubation, dishes were placed on the imaging incubator with 5% CO<sub>2</sub>, 37°C for cell live imaging. Live cell imaging was obtained for 2 h per 30 s using a Nikon Eclipse Ti2 fluorescent microscope (Tokyo, Japan). The acquired images were analyzed by Image J (36) and Volocity (PerkinElmer, Waltham, MA, USA).

### Immunofluorescence of *in vitro* NET formation

To detect released NETs *in vitro*, 2×10<sup>5</sup> neutrophils isolated from WT and NLRP3 KO mice bone marrow were seeded onto the surface of each well of a fibronectin-coated 8-well Cell Culture Chamber (SPL Life Sciences, Pocheon, Korea). Neutrophils were stimulated with 1 µg/ml *E. coli*-derived LPS and incubated for 3 h in 5% CO<sub>2</sub> at 37°C. Following incubation, neutrophils were stained with 5 µM SYTOX for 5 min at 25°C in the dark and rinsed gently with PBS. Stained neutrophils were fixed in 4% paraformaldehyde for 10 min and incubated with 1:500 anti-citrullinated histone H3 (CitH3, ab5103; Abcam, Cambridge, MA, USA) at 4°C overnight. The cells were washed in PBS the following day and incubated with 1:500 Alexa Fluor 488 goat anti-rabbit IgG (ab150077; Abcam) for 2 h, at 25°C in the dark. Prior to mounting, cells were stained with DAPI for 5 min. The slide was then covered with ProLong Diamond Antifade Mount solution (Thermo Fisher Scientific) and incubated for at least 1 day at 4°C until solidification. All the images were obtained with a Nikon Eclipse Ti2 fluorescent microscope using 20X and 60X objectives. NETs were identified by the co-localization of SYTOX and CitH3 as previously described (6), and 20X images were used for quantification.

The NET formation was observed and displayed using the 60X images. Fluorescent images were analyzed using Volocity (PerkinElmer) and Image J (36) software.

### Brain cell isolation

Leukocytes from the brain were acquired, as demonstrated previously (37). Briefly, Mice were perfused with PBS to eliminate intravascular cells, and harvested brain tissues were ground in 1X Hanks' balanced salt solution (HBSS; Thermo Fisher Scientific). Stock isotonic percoll (SIP) was prepared by mixing 10X HBSS and pure percoll (GE Healthcare, Little Chalfont, UK). Cell suspension solution was made to a final of 30% SIP. Over the top of 70% SIP, the cell suspension solution prepared to a final 30% SIP was stacked slowly to make a gradient layer. After centrifugation at 500 g for 30 min, a flat visible leukocyte cell belt was obtained at the 70%–30% junction. Collected cells were rinsed in 1X HBSS.

### Western blot

Brain tissues were harvested after perfusion from WT and NLRP3 KO mice in each PBS and LPS-injected group and ground using a strainer. The total proteins were obtained using PRO-PREP protein extraction solution (iNtRON Biotechnology, Seongnam, Korea) and analyzed following the previously used method (6). In brief, primary Abs, CitH3 (ab5103; Abcam), NLRP3 (# AG-20B-0014; AdipoGen, San Diego, CA, USA), and  $\beta$ -actin (#8457; Cell Signaling Technology, Boston, MA, USA), were used to detect the NET formation in the brain tissue. After overnight incubation with primary Abs, the membrane was incubated with a secondary Ab for 1 h at 25°C. The membrane was developed using Clarity Max Western ECL substrate (Bio-Rad, Hercules, CA, USA) and the ImageQuant LAS 4000 mini (Fujifilm, Tokyo, Japan). Each time, the membrane was rinsed thrice with TBS-T. The signals were quantified using Image J (36) software.

### Immunofluorescence of *in vivo* NET formation

Released NETs in mouse brain tissues were examined by immunofluorescence microscopy. The perfused brain tissues were fixed in fresh 4% paraformaldehyde solution at 4°C for 1 day. Fixed brain tissues stayed in 30% sucrose hypertonic solution until they sank and were embedded in optimal cutting temperature (38) compound. Cryo-embedded brain tissues were sectioned at 10  $\mu$ m thickness and washed thrice in PBS to remove unnecessary OCT compound. The tissues were permeabilized, and non-specific binding was blocked using 1% BSA, 2 mM EDTA, and 0.5% Triton X-100 in PBS for 1 h at 25°C. Subsequently, the tissues were incubated with primary Abs, CitH3 (ab5103; Abcam) and myeloperoxidase (MPO, ab208670; Abcam), at 4°C overnight. The slides were then rinsed in PBS and incubated with secondary Abs Alexa Fluor 488 goat anti-rabbit IgG 2  $\mu$ g/ml (ab150077; Abcam) and Alexa Fluor 555 goat anti-rabbit IgG 2  $\mu$ g/ml (ab150078; Abcam) in same media that was used for permeabilization for 2 h at 25°C. After rinsing thrice in PBS, the tissues were stained with DAPI. Images were obtained using Nikon Eclipse Ti2 fluorescent microscope and analyzed with Volocity (PerkinElmer) software according to previously demonstrated (6).

### Immunohistochemistry (IHC)

LPS-injected WT and NLRP3 KO mice brains were collected to evaluate *in vivo* brain damage. Tissue slides were prepared as described previously in immunofluorescence *in vivo* and sectioned 10  $\mu$ m for IHC staining. IHC staining was performed using the Novolink Polymer Detection System (RE7290-K; Leica Biosystems, Nussloch, Germany), according to the manufacturer's description. Briefly, the tissue slides were immersed in cold acetone for 10 min and washed with PBS. Next, peroxidase activity was neutralized with a peroxidase block

for 10 min. Then, slides were rinsed with PBS and treated with protein block for 1 h at 25°C. Following another PBS wash, tissue sections were incubated with primary ZO-1 (Cat# 40-2200; Invitrogen) and Claudin-5 (Cat# 35-2500; Invitrogen) Abs at 4°C overnight. Slides were rinsed with PBS and incubated with a secondary Ab for 2 h at 25°C. After washing the slides with PBS, novolink polymer was applied for 30 min. Rinsed slides were treated with a DAB working solution for 5 min. Samples were counterstained with novolink hematoxylin for 10 min, dehydrated and coverslipped.

### Flow cytometry

Isolated neutrophils were used to quantify the number of plasma membrane-damaged cells from WT and NLRP3 KO, treated with 1 µg/ml *E. coli*-derived LPS and incubated for 3 h in 5% CO<sub>2</sub> at 37°C. Cells were then collected and stained with 5 µM SYTOX-orange in the buffer for 5 min at 25°C in the dark. Stained cells were rinsed twice. SYTOX-positive neutrophils were identified as plasma membrane ruptured cells (33-35). We also conducted the neutrophil viability test to confirm the dead neutrophils which lead to NETosis. Neutrophils were stimulated with the same conditions as before and stained by the annexin V staining viability protocol (39,40). Briefly, stimulated total cells were harvested and incubated with FITC annexin V (BioLegend, San Diego, CA, USA) and propodeum iodide (PI) (Thermo Fisher Scientific) solution for 15 min at 25°C in the dark. Dead neutrophils were identified as annexin V and PI double-positive population. To determine the number of infiltrated neutrophils in the brain under systemic inflammation, we injected 2.5 mg/kg *E. coli*-derived LPS intravenously into WT mice. We perfused mice before sacrifice and harvested the brain 6 h and 24 h post-injection. Besides, we compared the number of infiltrated neutrophils after 24 h in NLRP3 absence. Leukocytes in the brain were obtained following the percoll cell gradient. Obtained cells were stained with CD11b-APC (BioLegend) and Ly6G-PE (BioLegend) for cell staining. CD11b and Ly6G double-positive cells were identified as neutrophils. At the 24 h LPS post-injection condition for NET formation *in vivo*, perfused brain tissues were harvested, and blood was collected from each WT, NLRP3 group LPS-injected mice. Obtained cells from the brain and blood were stained with Ly6G (Cat# 127607; BioLegend), CitH3 (Cat# ab5103; Abcam), and MPO (Cat# ab90812; Abcam) to quantify NET formation in the brain (9). Alexa 647 anti-rabbit IgG (Cat# 406414; BioLegend) Abs were used for fluorescence labeling on the unconjugated Ab. Samples were acquired on an LSRII (BD Biosciences, Franklin Lakes, NJ, USA) and analyzed using FlowJo software (FlowJo, LLC, Ashland, OR, USA).

### Two-photon imaging of mouse brain

Two-photon imaging was performed to observe NET formation in the mouse brain after 24 h of 2.5 mg/kg, intravenous (i.v.) LPS injection. An anesthetized mouse was placed in a customized chamber, and the brain surgery was conducted prior to imaging as previously described (41,42). NET-defining markers, which are NE Ab Alexa Fluor 488 (Ssc-55549 AF488; Santa Cruz Biotechnology, Santa Cruz, CA, USA) and CitH3 (Cat# ab5103; Abcam), were intravenously inoculated to visualize the NET formation. For the fluorescence imaging of NETs, the CitH3 Ab was conjugated to Alexa Fluor 594 using Ab labeling kits, as per the manufacturer's instructions (Invitrogen). The blood vessel was visualized by injecting wheat germ agglutinin (WGA) (Cat# 29028; Biotium, Eching, Germany). Acquired Images were analyzed with Volocity, Image J, and Imaris based on previous reports (18).

### Neutrophil depletion

Anti-Ly6G-mediated neutrophil depletion in mice was performed by the administration of 4 mg/kg of the anti-Ly6G Ab (clone 1A8; BioLegend) twice at a 24 h interval via intraperitoneal injection. The neutrophil depletion process was initiated 24 h prior to LPS injection to ensure adequate depletion of neutrophils. Mice brains were harvested 24 h after the administration of 2.5 mg/kg of *E. coli*-derived LPS intravenously. The efficiency of neutrophil depletion was assessed by evaluating changes in immune cell populations in the brain using previously established protocols (43,44).

### Measurement of cytokines level

The secretion levels of the inflammatory cytokines TNF- $\alpha$  and IL-1 $\beta$  were measured using an ELISA (R&D Systems, Minneapolis, MN, USA), following the manufacturer's instructions. Total whole-brain proteins and cell supernatants were used and were triplicated to assay the cytokine levels. The quantification of IL-1 $\beta$  and TNF- $\alpha$  levels was expressed as picograms of cytokine per milligram of protein (pg/mg protein).

### Statistical analysis

All data were expressed as mean  $\pm$  SEM. A comparison of the 2 groups was performed using a 2-tailed Student's *t*-test. More than 3 groups were compared via a one-way analysis of variance (45). Statistical significance was set to  $p < 0.05$ . GraphPad Prism Software (version 7.00; GraphPad, CA, USA, www.graphpad.com) was used for all statistical analyses, and the results were derived from at least the triplicate of experiments.

## RESULTS

### NLRP3 facilitated neutrophil plasma membrane breakdown as the prerequisite for DNA leakage

In the process of NET formation, neutrophils secrete intracellular proteins along with DNA. Plasma membrane breakdown is essential to eject internal molecules, especially DNA, during the process. Therefore, we investigated whether NLRP3 is involved in plasma membrane rupture. We exploited SYTOX, an impermeable DNA dye, to observe the plasma membrane destruction, in which SYTOX can only stain DNA that is not membrane-enclosed (33-35). To determine the optimal LPS concentration for neutrophil stimulation in SYTOX staining, we tested 0.01, 0.1, and 1  $\mu\text{g/ml}$  *E. coli*-derived LPS based on previous reports (6,46-48). Owing to the short-life span of neutrophils, they were cultured for 1 h and 3 h on each concentration to find the optimal condition for live imaging. Induction with 1  $\mu\text{g/ml}$  LPS and culturing for 3 h proved to be the optimal conditions for viewing the real-time plasma membrane breakdown. We also confirmed that the NLRP3 inflammasome is activated, and IL-1 $\beta$  is secreted after 3 h of 1  $\mu\text{g/ml}$  LPS treatment. This result shows that the setup condition is proper for studying the role of the NLRP3 inflammasome (**Supplementary Fig. 1**). To address the role of NLRP3 in plasma membrane rupture, we compared the SYTOX-positive intensity of WT and NLRP3 KO neutrophils cultured in these selected stimulation conditions. First, isolated neutrophils were activated with 1  $\mu\text{g/ml}$  LPS and treated with 5  $\mu\text{M}$  SYTOX for 1 h. We performed live cell imaging from 1–3 h after stimulation (**Fig. 1A**). We found that WT neutrophils exhibited relatively rapid plasma membrane breakdown and stronger SYTOX intensity compared to NLRP3 KO as time progressed (**Fig. 1B and C**). A fluorescent image at the 2 h time-point following LPS stimulation showed fewer SYTOX-stained cells in NLRP3 KO neutrophils (**Fig. 1D**). Furthermore, we inspected the difference in the SYTOX-positive cell population in the absence of NLRP3

at 3 h of 1  $\mu\text{g/ml}$  LPS stimulation. Consistent with the previous result, the WT neutrophil population contained significantly more SYTOX positive cells than NLRP3 KO upon LPS stimulation, according to Flow cytometry quantification (Fig. 1E and F). However, there was no endogenous difference in SYTOX-positive staining in WT and NLRP3 KO PBS-treated groups. These results suggest that NLRP3 promotes plasma membrane rupture and can

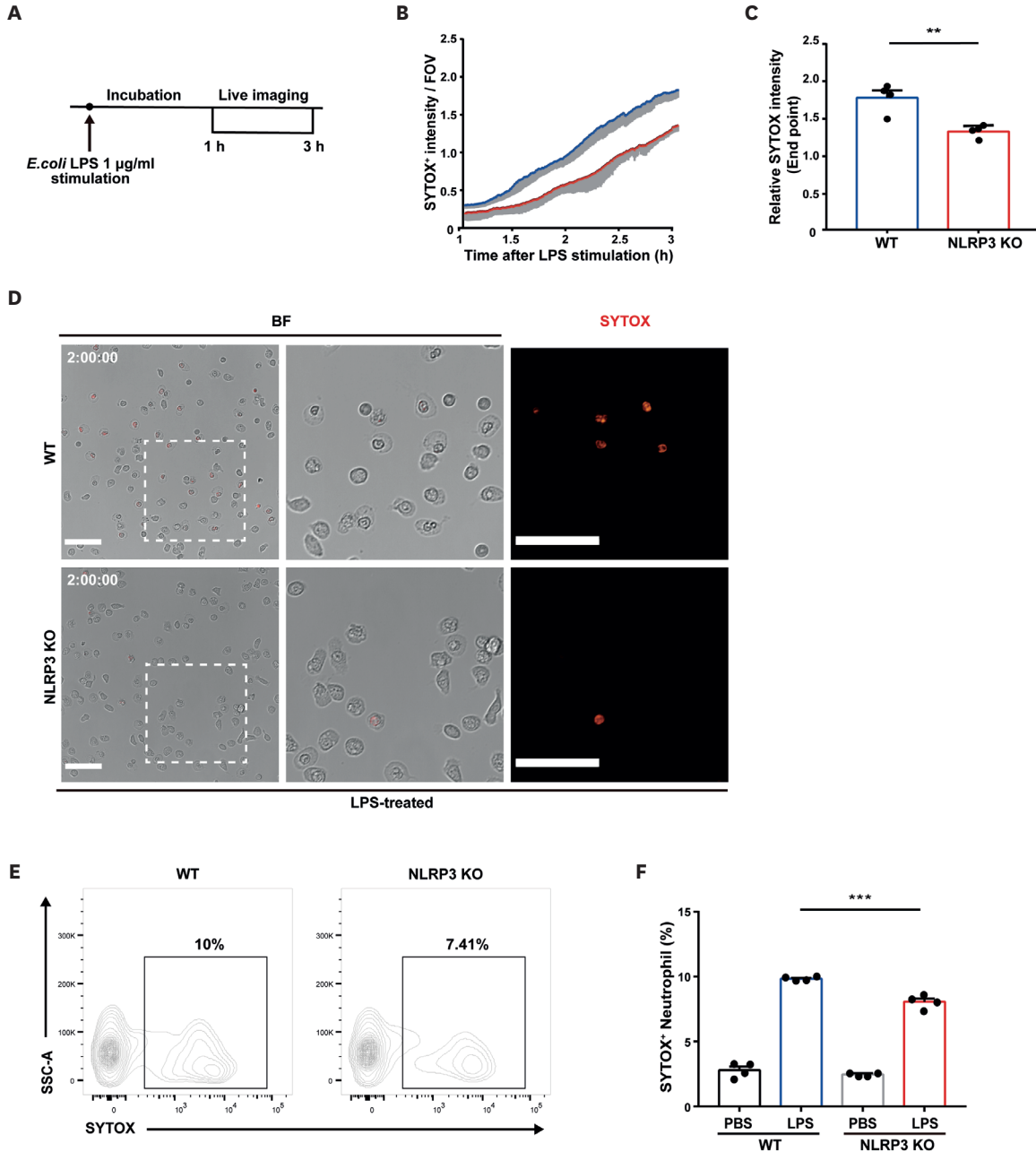


**Figure 1.** NLRP3 promotes DNA leakage from neutrophils.

(A) Scheme of live cell imaging in WT and NLRP3 KO mice neutrophils in the presence of SYTOX and LPS. Given conditions were treated with LPS (1  $\mu\text{g/ml}$ ) and SYTOX-orange (red, 5  $\mu\text{M}$ ). Live imaging was performed from 1–3 h after LPS stimulation. (B–D) SYTOX staining indicated DNA leakage with bright orange fluorescence. (B) Relative SYTOX signal with time progression (C) quantitative comparison at the endpoint at 3 h after LPS stimulation. (D) Fluorescence SYTOX-orange (red) staining images of WT and NLRP3 KO neutrophils at 2 h after LPS stimulation (scale bars=50  $\mu\text{m}$ ). (E, F) The number of SYTOX-positive cells in WT and NLRP3 KO neutrophils after 3 h of LPS stimulation by flow cytometry. (E) Representative LPS-treated neutrophils in WT and NLRP3 KO group (F) quantitative demonstration of membrane-cleaved cells. All experiments were independently repeated at least 3 times. \*\* $p < 0.01$ , \*\*\* $p < 0.001$ .

create a preferential environment for NET formation via expediting DNA leakage, particularly upon LPS stimulation.

**NLRP3 elevated NET formation accompanied by neutrophil death; NETosis**

Next, we assessed whether NLRP3 plays a further crucial role in NET formation apart from the increased plasma membrane destruction. NET formation was initially known as a host defense function of neutrophils to trap and kill pathogens (3). Excessive NET formation, however, can be an etiological factor and cause deleterious tissue damage (6,18). Thus, neutrophils from WT and NLRP3 KO mice were stained with NET-specific indicators SYTOX and CitH3 to detect the extracellular DNA and the citrullinated histones present in NETs. We employed CitH3 as the main hallmark of NETs, which results from chromatin decondensation and the conversion of arginine to citrulline (13,47,49,50). We found that SYTOX- and CitH3-stained cells were significantly reduced in the absence of NLRP3, compared to WT (Fig. 2A). In addition, stained regions indicating SYTOX and CitH3 co-localization were much less in the absence of NLRP3 compared to WT (Fig. 2B). It has been reported that there are 2 NET formation pathways, namely, suicidal and vital (12). To specify which pathway is supported by NLRP3 in the LPS stimulation, we tested the viability of neutrophils under the same conditions. The results revealed that NLRP3 supports neutrophil death upon a 3 h stimulation by 1 µg/ml *E. coli*-derived LPS (Fig. 2C-E). Therefore,

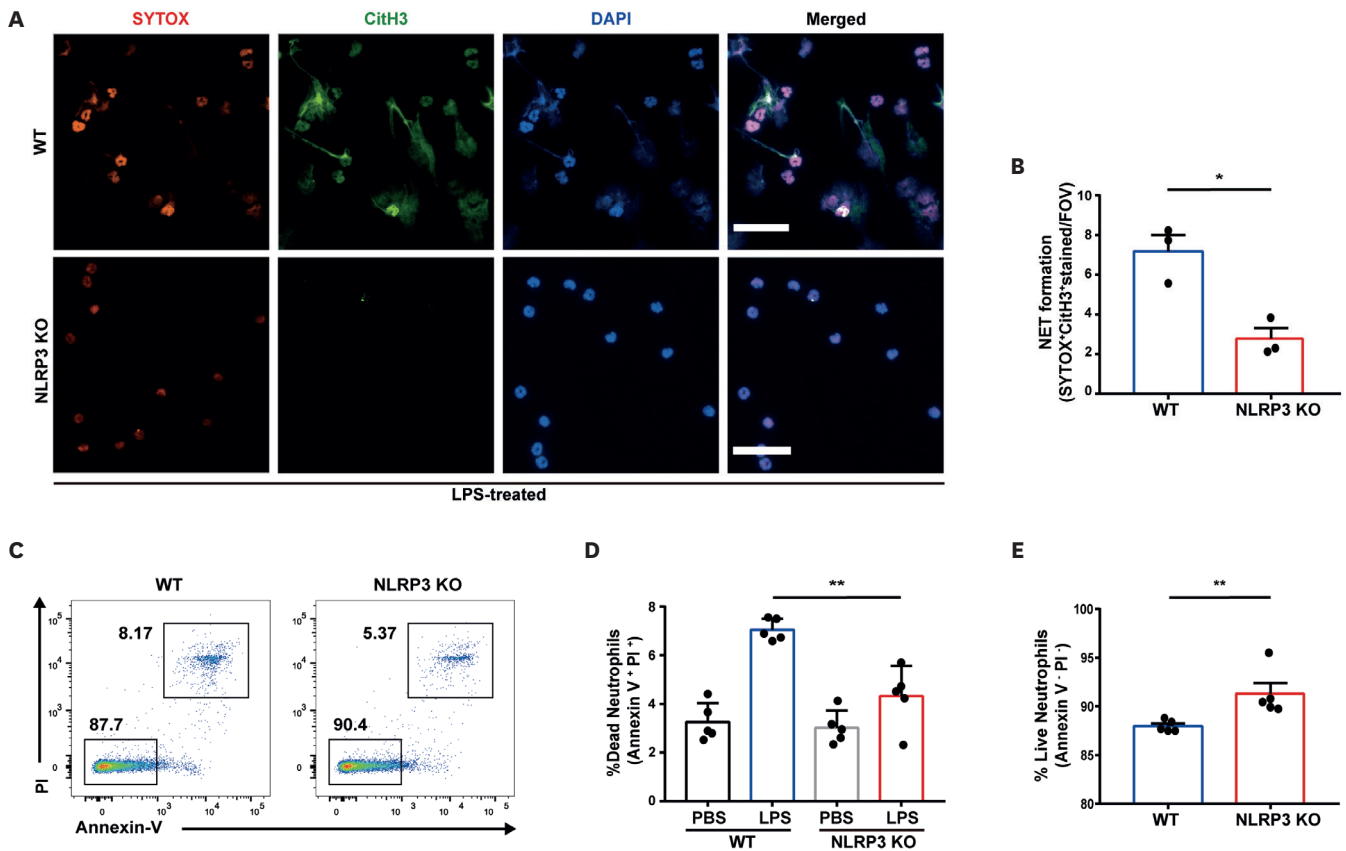


**Figure 2.** NLRP3 elevates NET formation and induces neutrophil death. (A) Representative fluorescent images of NET formation by staining with SYTOX-orange (red), CitH3, and nuclei (blue) in WT and NLRP3 KO neutrophils stimulated with 1 µg/ml of LPS for 3 h (B) quantitative demonstration of NET formation with SYTOX and CitH3 co-localization (scale bars=50 µm). (C-E) Viability test of WT and NLRP3 KO neutrophils after stimulation with 1 µg/ml of LPS for 3 h. (C) Representative and (D) quantitative comparison of annexin V and PI double-positive (dead) neutrophils in WT and NLRP3 KO neutrophils by flow cytometry. (E) Annexin V and PI double-negative live neutrophils under LPS stimulation. All results represent findings from at least 3 independent experiments. \*p<0.05, \*\*p<0.01.

these results implicate NLRP3 in NET formation, accompanied by neutrophil death, which suggests that NLRP3 aids suicidal NET formation; NETosis.

**Neutrophil infiltration was independent of NLRP3 in the acute inflammatory environment of brain**

To gain insight into the role of NLRP3 in the neutrophil function in the inflamed brain, we set up the neuroinflammation model by comparing the number of infiltrated neutrophils. It has been well established that LPS-induced septic conditions cause inflammatory environment in the brain by peripheral stimulation and induce neutrophil infiltration to the brain (29-31,51,52). Thus, we injected 2.5 mg/kg *E. coli*-derived LPS intravenously and observed the differences in infiltrated neutrophils. We set short time-periods, 6 h and 24 h post the i.v. injection of LPS, since the neutrophil-related reaction is an early stage of innate immune response, including NET formation, which especially can also be eliminated by other phagocytes subsequently. From the isolated brain leukocytes, neutrophils were identified as the CD11b and Ly6G double-positive population. Our results delineated that 2.5 mg/kg of LPS administration for 24 h is optimal for studying neuropathology in our study design (Fig. 3A and B). With the chosen conditions, we next explored whether the absence of NLRP3 could lead to different levels of neutrophil infiltration in the brain. Interestingly, the number of infiltrated neutrophils was indistinguishable between WT and NLRP3 KO in LPS-induced neuroinflammation (Fig. 3C and D). These findings provide a hypothesis that NLRP3 may not have an impact on neutrophil infiltration but could influence NET formation.

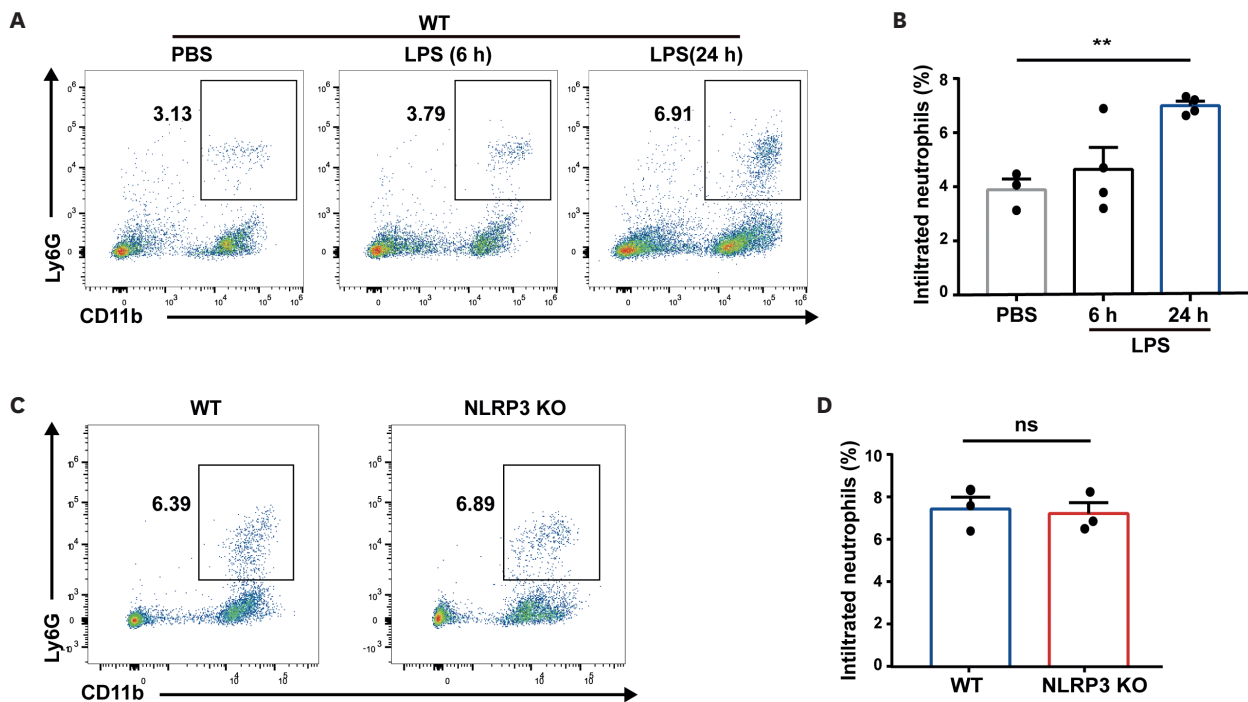


**Figure 3.** NLRP3 deficiency does not affect the amount of neutrophil infiltration in neuroinflammation. (A, B) Comparison of the number of infiltrated neutrophils in the brain post 6 h and 24 h of 2.5 mg/kg LPS injection performed intravenously in WT mice. Infiltrated Neutrophils in the brain were sorted using CD11b and Ly6G staining (B) quantitative demonstration by flow cytometry. (C) Flow cytometry analysis of the number of infiltrated neutrophils in the brains of WT and NLRP3 KO at 24 h following LPS injection (D) quantitative comparison of infiltrated neutrophil number. All data are representative of experiments repeated more than thrice. \*\*p<0.01.

### The absence of NLRP3 alleviated NETosis in the inflamed mouse brain

We next sought to check if NLRP3 deficiency affected the neutrophil function of NET formation in the inflamed brain. Given that there was no difference in the number of infiltrating neutrophils in the brains of WT and NLRP3 KO mice (**Fig. 3C and D**), we focused on the NET formation ability of neutrophils under the absence of NLRP3 in the brain. To this end, we used the same mouse model of LPS-induced neuroinflammation to delineate the differences in NET formation and thus harvested brains from WT and NLRP3 KO mice for several analysis sessions (**Fig. 4A**). We first evaluated CitH3 expression, one of the well-known NET indicators, at the protein level in the brain using Western blotting (13,49,50). The marked difference in CitH3 protein levels in PBS- and LPS-treated WT mice further validated that our mouse model of LPS-induced neuroinflammation is optimal for studying NET formation in the brain. By contrast, NLRP3 deficiency resulted in reduced CitH3 expression under the same conditions (**Fig. 4B and C**). In the same context, histological fluorescence examination of the mouse brains revealed that in the absence of NLRP3, the expression of CitH3 and MPO, which are significant sub-molecules involved in NET formation, was decreased (**Fig. 4D**). Consistent with these findings, we investigated CitH3 and MPO double-positive neutrophils in the brain to quantify NET formation via flow cytometry as previously reported (9,53,54). The proportion of NET formation, identified as Ly6G<sup>+</sup>CitH3<sup>+</sup>MPO<sup>+</sup>, was significantly diminished in the LPS-injected brain of NLRP3 KO mice compared with WT mice (**Fig. 4E and F**). However, circulating NETs were not affected in the absence of NLRP3 (**Fig. 4G and H**). In addition, we tested the viability of brain-infiltrated neutrophils to identify whether NLRP3-dependent NET formation undergoes suicidal NET formation; NETosis, as we observed previously *in vitro* (55). We gated Ly6G-positive brain-infiltrated neutrophils and compared the number of dead neutrophils between the WT and NLRP3 groups. The results indicate that NLRP3 supports NETosis in the inflamed brain. Our results collectively suggest that NLRP3 deficiency limits NETosis, especially in the inflamed brain, possibly alleviating the deleterious effect of excessive accumulation of NETs.

### NLRP3-deficient mice exhibited the reduction NET formation as observed in two-photon imaging

To more accurately understand NET formation as sustained by NLRP3, we performed two-photon imaging in LPS-injected WT and NLRP3 KO mice under the designed *in vivo* conditions (**Fig. 4A**). We utilized NE and CitH3 to visualize the NET components in live mice brains as previously described (56-59). NE is an endogenous enzyme characteristically found in the NET structure similar to MPO. NLRP3 KO mice brains showed a conspicuously decreased CitH3-stained area compared to WT (**Fig. 5A-C**). In addition, the NE-stained region showed the same tendency with CitH3; decreased in NLRP3-deficient mice brains. Taken together, NLRP3 can cause excessive NET formation in the inflamed brain, as indicated by experiments in living animals as well.

### NLRP3 deficiency attenuated inflammatory state in the inflamed brain

To identify the degree of neuroinflammation under lessened NET formation by the NLRP3 deficiency, we evaluated BBB breakdown as one of the main characteristics of neuroinflammation. The BBB is a central and unique structure present in the brain that makes the brain an immune-privileged organ. This structure normally exists intact and plays a role in protecting the brain from invading pathogens or immune cells. However, when inflammation occurs in the brain, the integrity of the BBB is lost, and the tight junction loosens, allowing immune cells to infiltrate the brain and become susceptible to all pathogens (29-31). Therefore, we compared the degree of BBB damage between WT and NLRP3 KO by evaluating

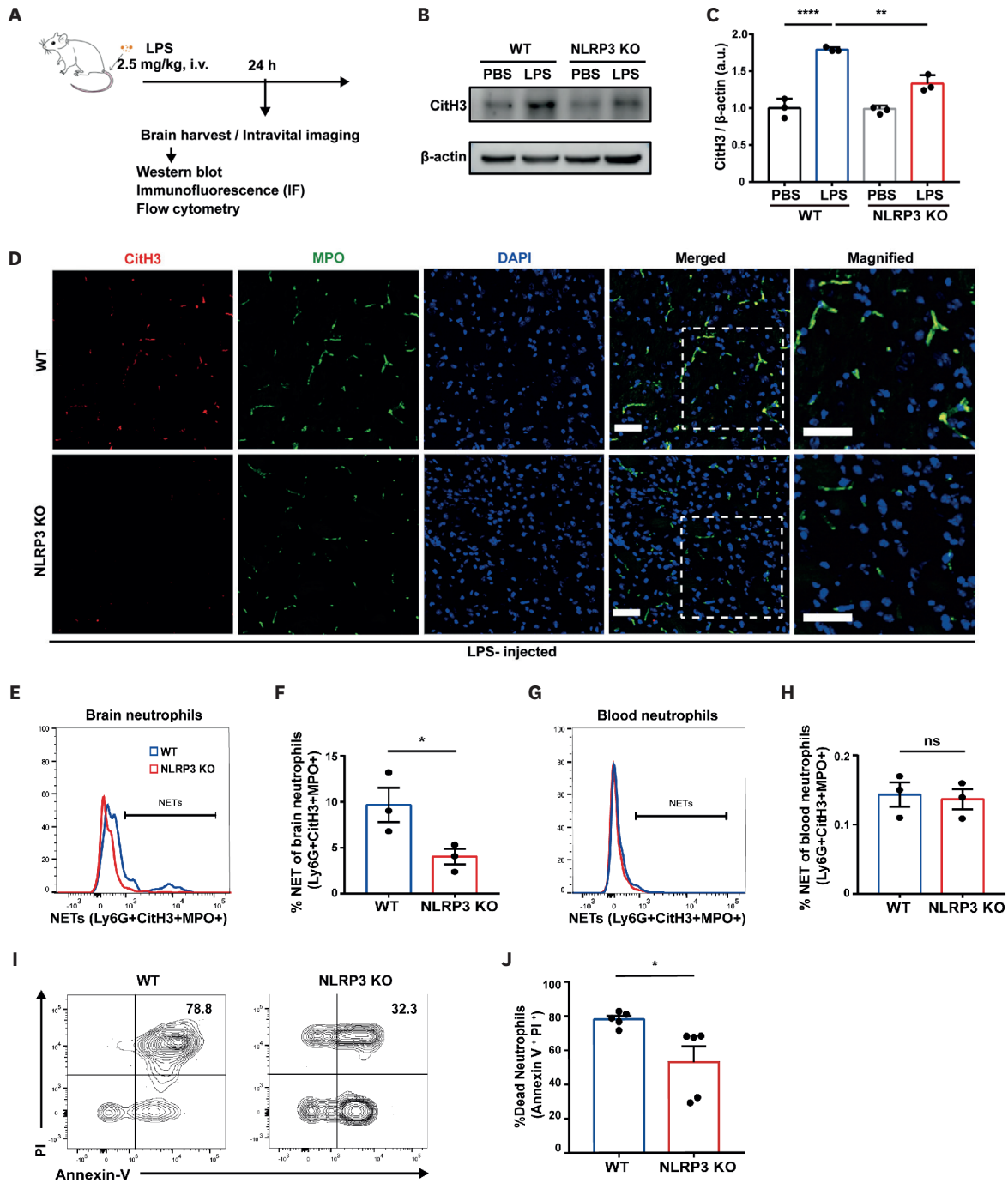


**Figure 4.** NLRP3 accelerates NET formation in the inflamed brain.

(A) Scheme of experimental design *in vivo*. (B) Representative cropped western blots of CitH3 and  $\beta$ -actin with proteins extracted from the whole brain tissues. (C) CitH3 production, as analyzed from Western blots done in triplicate (B) was normalized over  $\beta$ -actin in WT and NLRP3 KO brain. (D) Representative Immunohistochemistry images of brain sections showing NET formation in LPS-injected WT and NLRP3 KO mice. CitH3 (red) and MPO were used as NET indicators, and DAPI (blue) for nuclei staining (scale bar=100  $\mu$ m). (E-H) Extracellular expression of CitH3 and MPO in Ly6G<sup>+</sup> neutrophils derived from the brain and blood of WT and NLRP3 KO mice after LPS injection. (E) Representative flow cytometry analysis of Ly6G<sup>+</sup> CitH3<sup>+</sup> MPO<sup>+</sup> co-expression in brain neutrophils; NET formation (F) quantitative evaluation of WT and NLRP3 KO. (G) Representative (H) quantitative comparison of NET formation from blood neutrophils; circulating NETs in WT and NLRP3 KO after LPS injection. (I) Representative and (J) quantitative comparison of annexin V and PI double-positive (dead) neutrophils in WT and NLRP3 KO brain infiltrated neutrophils via flow cytometry. All results shown are from 3 independent experiments. \* $p < 0.05$ , \*\* $p < 0.01$ , \*\*\*\* $p < 0.0001$ .

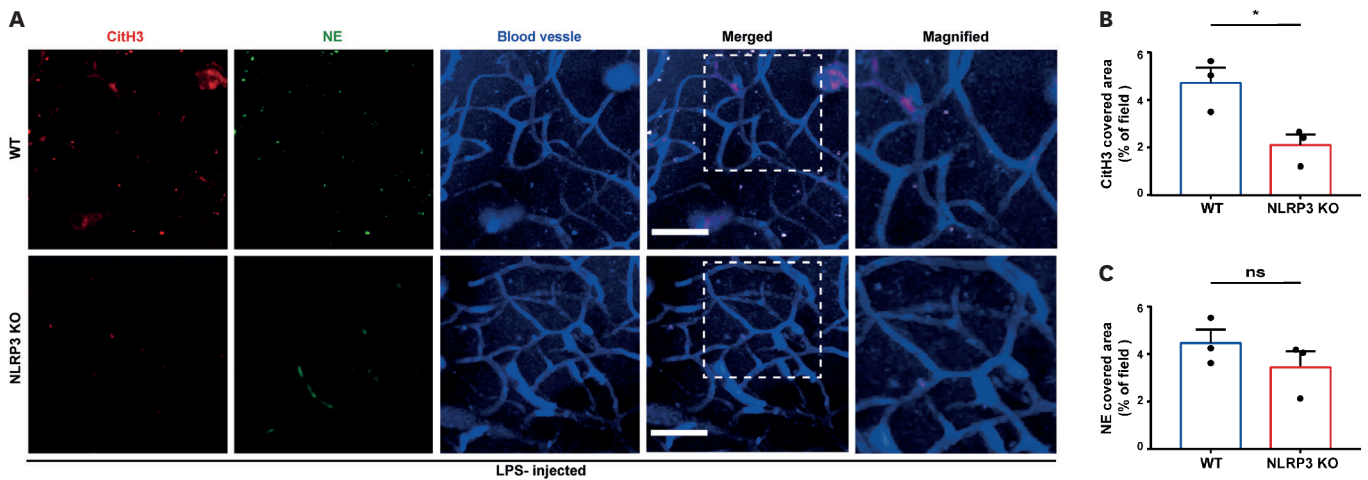


**Figure 5.** Two-photon deep tissue observation of diminished NET formation in NLRP3-deficient mice brains.

(A) Representative images of NET formation obtained from two-photon imaging of WT and NLRP3 KO mice. Mice were injected with 2.5 mg/kg LPS 24 h prior to imaging. NET components CitH3, stained with Alexa-594 anti CitH3 Ab (red) and Alexa 488-conjugated NE, blood vessels were labeled with WGA (blue). Quantitative analysis of NETs in the brain of mice systemically injected with LPS; (B) area of CitH3 and (C) of NE staining (scale bar=50  $\mu$ m). Data represent findings from experiments repeated thrice. \*p<0.05.

the expression of Claudin-5 and Zonula Occludens-1 (ZO-1), which are tight junction-associated proteins that determine the integrity of the BBB via histological analysis (38,60-62). Claudin-5 and ZO-1 are proteins that express a certain amount in endothelial cells in the intact state brain. However, when the integrity of the tight junction of the BBB is broken, the expression level decreases. We confirmed that the expression of Claudin-5 and ZO-1 are both reduced in the inflamed brain via immunohistochemistry (Fig. 6A-C). We compared to WT, NLRP3 KO mice brain tissue showed more intact Claudin-5 and ZO-1 stained structures. Additionally, we estimated the expression level of TNF- $\alpha$  and IL-1 $\beta$ , well-known inflammatory cytokines, in the whole brain tissue lysate. The result determines NLRP3-deficiency alleviates both pro-inflammatory cytokines (Fig. 6D and E). This result implicates NLRP3 supports NET formation in the inflamed brain and leads to brain damage.

### Inhibition of NET formation through neutrophil depletion relieved inflammatory state in the brain

We investigated whether the reduction of NET formation is responsible for alleviating inflammatory status in NLRP3-deficient mice. To eliminate the possibility of NET formation, we depleted neutrophils using anti-Ly6G treatment. In this way, we confirmed the elimination of brain-infiltrating neutrophils (Supplementary Fig. 2) (41,42). We then measured changes in the expression of tight junction-associated proteins to assess BBB integrity following neutrophil depletion. Our results showed that neutrophil depletion increased the expression of Claudin-5 and ZO-1 in the inflamed brain, indicating that ablation of possible NET formation alleviates BBB damage (Fig. 7A-C). We also evaluated the concentration of IL-1 $\beta$  and TNF- $\alpha$ . The production level of IL-1 $\beta$  was lower in the neutrophil-depleted inflamed brain than that in the LPS-injected inflamed brain alone (Fig. 7D). However, anti-Ly6G treatment did not affect the production level of TNF- $\alpha$  (Fig. 7E). Therefore, excessive NETosis supported by NLRP3 worsens neuroinflammation, aggravating BBB damage and escalating the expression of the pro-inflammatory cytokine IL-1 $\beta$ . These results suggest that the deficiency of NLRP3 induces less NET formation, which could ultimately be applied clinically to attenuate brain damage.

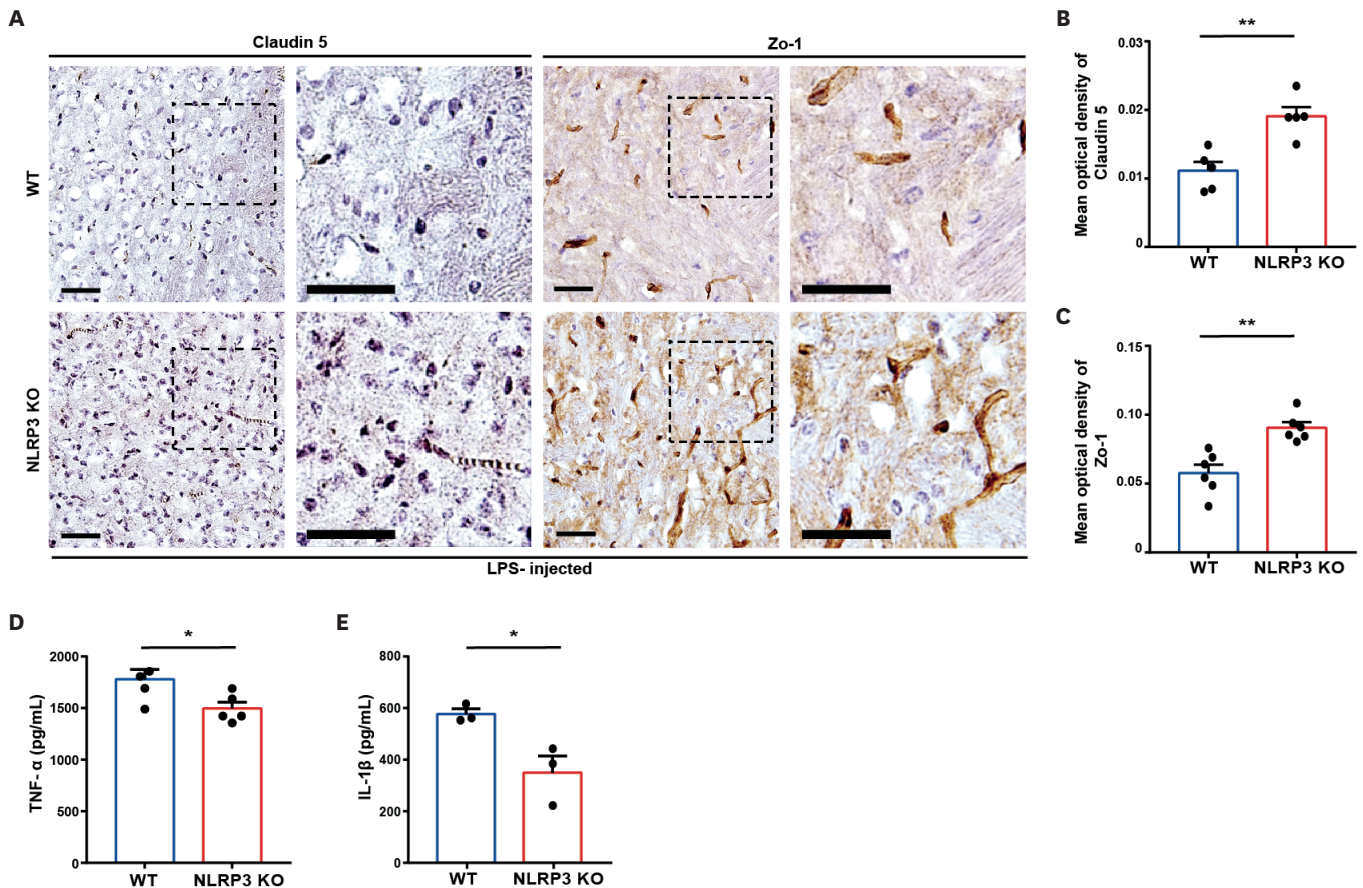


**Figure 6.** NLRP3-deficiency attenuates neuroinflammation in inflamed mice brains.

(A) Representative images of IHC obtained from WT and NLRP3 KO mice brains by staining with ZO-1 and Claudin-5. Mice were injected with 2.5 mg/kg LPS 24 h before harvest and perfused with PBS. BBB tight junction-associated proteins, ZO-1 and Claudin-5, were labeled in 10 μm sectioned brain tissues. Quantitative analysis of ZO-1 and Claudin-5 expression in the brain; (B) area of Claudin-5 and (C) of ZO-1 staining (scale bar=50 μm). Inflammatory cytokine level was evaluated with whole brain lysates after 24 h of 2.5 mg/kg LPS injection in WT and NLRP3 KO groups. (D) TNF-α and (E) IL-1β concentration were detected with ELISA. Data represent findings from experiments repeated at least 3 times.

\*p<0.05, \*\*p<0.01.

## DISCUSSION

The secretion of NETs was previously viewed as a host defense function of neutrophils, capturing the pathogen. However, after the possible deleterious effect of NETs was highlighted, NETs were regarded as a double-edged sword (15,42). Recently the overall role of NETs leans more towards the toxic effect. NETs have sticky properties that can not only trap the pathogen but also easily aggregate and accumulate in the inflamed site. In addition, the ejected NET components can promote an inflammatory state and make the tissue susceptible to damage (18). Several previous studies revealed that NETs are linked to various neurological diseases (7). Herein, we focused on NLRP3, a reliable molecule in NET formation with evident expression in the neutrophils, which was also studied in several NET-related diseases (10,24).

We found that NLRP3 facilitates DNA leakage and NET formation in neutrophils under LPS stimulation and further confirmed that endogenous cell viability by itself is not the cause, as indicated by the results from the PBS-treated group. Moreover, NLRP3 did not affect the number of infiltrating neutrophils in the inflammatory environment induced by LPS under the experimental conditions chosen in our study. Thus, we identified that even though

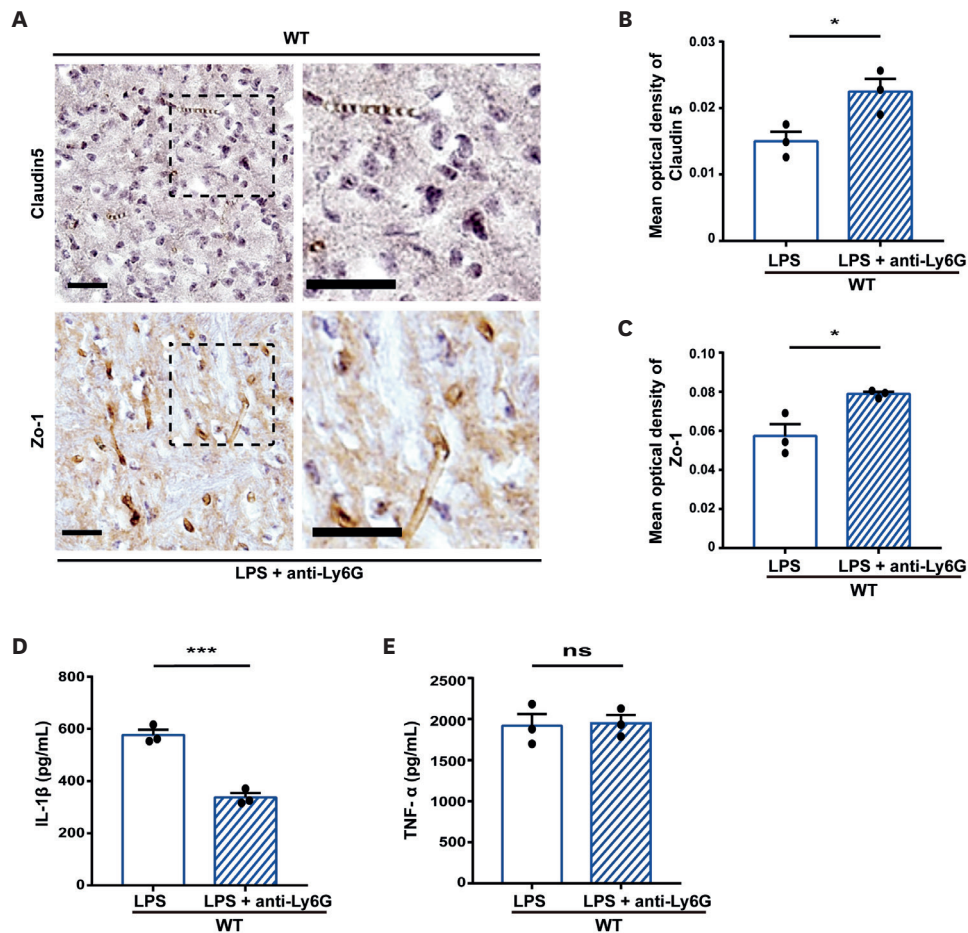


**Figure 7.** NET inhibition via neutrophil depletion alleviates neuroinflammation in the inflamed brain.

Mice were treated with 4 mg/kg of anti-Ly6G twice; Anti-Ly6G was administered 24 h prior to LPS injection. As a second injection, anti-Ly6G was administered simultaneously with 2.5 mg/kg of LPS. Mice brains were harvested 24 h after LPS injection. (A) Representative IHC images of staining with ZO-1 and Claudin-5 were obtained from anti-Ly6G-treated WT mice. Quantitative analysis of ZO-1 and Claudin-5 expression in the brains of mice treated with only LPS and LPS with anti-Ly6G; (B) area of Claudin-5 and (C) of ZO-1 staining (scale bar=50  $\mu$ m). (D) IL-1 $\beta$  and (E) TNF- $\alpha$  expression levels were detected with ELISA. Data represent findings from experiments repeated thrice.

\* $p < 0.05$ , \*\*\* $p < 0.001$ .

the same number of neutrophils infiltrated the inflamed brain, the number of neutrophils emitting the NETs can be different in the absence of NLRP3. Furthermore, we confirmed that the lack of NLRP3 could mitigate the neuroinflammatory state, which is identified as BBB damage and pro-inflammatory cytokine expression. We clarified the aggravation of BBB damage and inflammatory cytokine expression is the direct consequence of NETosis through indirect ablation of NET formation. Interestingly, although NLRP3 deficiency diminished both TNF- $\alpha$  and IL-1 $\beta$  levels in the inflamed brain, neutrophil depletion decreased only IL-1 $\beta$  levels but not TNF- $\alpha$ . Therefore, we concluded that the primary source of decreased IL-1 $\beta$  was neutrophils. In other words, NLRP3 inflammasome augments neuroinflammation via excessive NETosis, which is mediated by IL-1 $\beta$ . Hypothetically, our findings suggest the existence of a possible positive feedback loop between NLRP3 inflammasome activation and NET formation, where the activated NLRP3 inflammasome produces mature IL-1 $\beta$ . This secreted IL-1 $\beta$  then stimulates neutrophils to generate more NETs, triggering NLRP3 inflammasome inside the neutrophil and leading to further IL-1 $\beta$  production. Several published references lend support to the idea of this positive feedback loop (1,11,63).

Consequently, our findings suggest that NLRP3 activation promotes NETosis-associated neuroinflammation, leading to aggravation of BBB damage and IL-1 $\beta$  production. This result has potential implications for several neuroinflammatory diseases where BBB disruption and IL-1 $\beta$  secretion have been implicated, such as multiple sclerosis, Alzheimer's disease, and stroke (64-66). Previous studies have reported the excessive presence of NETs in the cerebrospinal fluid and brain lesions of patients with multiple sclerosis and Alzheimer's disease compared to the healthy group (7,67,68). Our study further proves that targeting NLRP3 and NETosis could be a novel therapeutic strategy for these neuroinflammatory diseases. Furthermore, our results suggest that IL-1 $\beta$  secretion via NLRP3 activation could be an early biomarker for these diseases, allowing for earlier diagnosis and treatment. Further investigation is warranted to explore the potential clinical applications of our findings.

While our findings suggest that NLRP3 has a pro-inflammatory role in the mouse brain mediated by excessive NET formation, it is important to note that there are contradictory findings regarding the inflammatory role of NLRP3. For example, NLRP3-deficient mice exhibited more severe and earlier herpetic stromal keratitis lesions during herpes simplex virus type 1 ocular infection, with increased inflammatory cytokine production and neutrophil infiltration (69). Therefore, the restraint of NLRP3 in the inflamed brain may have multiple possible side effects since NLRP3 has versatile functions and is involved in several endogenous cellular mechanisms. Hereby, it is essential to carefully consider the potential risks and benefits of NLRP3 inhibition and further elaborative investigation of NLRP3-involved physiological functions. In summary, our findings suggest that NLRP3 activation promotes NETosis-associated neuroinflammation, leading to aggravation of BBB damage and IL-1 $\beta$  production. Our study implies NLRP3 as a potential molecular target for developing therapeutic strategies to alleviate neuroinflammation in various neuroinflammatory diseases.

## ACKNOWLEDGEMENTS

We thank the imaging core facility at Yonsei University College of Medicine for supplying the two-photon microscope.

This work was supported by a grant from the Myung-Sun Kim Memorial Foundation to Young-Min Hyun (#2021).

## SUPPLEMENTARY MATERIALS

### Supplementary Figure 1

NLRP3 inflammasome is activated under 3 h of 1  $\mu$ g/ml LPS stimulation.

[Click here to view](#)

### Supplementary Figure 2

Anti-Ly6G treatment depletes neutrophil infiltration to the brain.

[Click here to view](#)

## REFERENCES

1. Bonaventura A, Vecchié A, Abbate A, Montecucco F. Neutrophil extracellular traps and cardiovascular diseases: an update. *Cells* 2020;9:9.  
[PUBMED](#) | [CROSSREF](#)
2. Hyun YM, Hong CW. Deep insight into neutrophil trafficking in various organs. *J Leukoc Biol* 2017;102:617-629.  
[PUBMED](#) | [CROSSREF](#)
3. Brinkmann V, Reichard U, Goosmann C, Fauler B, Uhlemann Y, Weiss DS, Weinrauch Y, Zychlinsky A. Neutrophil extracellular traps kill bacteria. *Science* 2004;303:1532-1535.  
[PUBMED](#) | [CROSSREF](#)
4. Barnes BJ, Adrover JM, Baxter-Stoltzfus A, Borczuk A, Cools-Lartigue J, Crawford JM, Daßler-Plenker J, Guerci P, Huynh C, Knight JS, et al. Targeting potential drivers of COVID-19: neutrophil extracellular traps. *J Exp Med* 2020;217:e20200652.  
[PUBMED](#) | [CROSSREF](#)
5. Saffarzadeh M. Neutrophil extracellular traps as a drug target to counteract chronic and acute inflammation. *Curr Pharm Biotechnol* 2018;19:1196-1202.  
[PUBMED](#) | [CROSSREF](#)
6. Jeong S, Kim B, Byun DJ, Jin S, Seo BS, Shin MH, Leem AY, Choung JJ, Park MS, Hyun YM. Lysophosphatidylcholine alleviates acute lung injury by regulating neutrophil motility and neutrophil extracellular trap formation. *Front Cell Dev Biol* 2022;10:941914.  
[PUBMED](#) | [CROSSREF](#)
7. Guo Y, Zeng H, Gao C. The role of neutrophil extracellular traps in central nervous system diseases and prospects for clinical application. *Oxid Med Cell Longev* 2021;2021:9931742.  
[PUBMED](#) | [CROSSREF](#)
8. Perez-de-Puig I, Miró-Mur F, Ferrer-Ferrer M, Gelpi E, Pedragosa J, Justicia C, Urrea X, Chamorro A, Planas AM. Neutrophil recruitment to the brain in mouse and human ischemic stroke. *Acta Neuropathol* 2015;129:239-257.  
[PUBMED](#) | [CROSSREF](#)
9. Vaibhav K, Braun M, Alverson K, Khodadadi H, Kutiyawalla A, Ward A, Banerjee C, Sparks T, Malik A, Rashid MH, et al. Neutrophil extracellular traps exacerbate neurological deficits after traumatic brain injury. *Sci Adv* 2020;6:eaax8847.  
[PUBMED](#) | [CROSSREF](#)
10. Campos J, Ponomaryov T, De Prendergast A, Whitworth K, Smith CW, Khan AO, Kavanagh D, Brill A. Neutrophil extracellular traps and inflammasomes cooperatively promote venous thrombosis in mice. *Blood Adv* 2021;5:2319-2324.  
[PUBMED](#) | [CROSSREF](#)
11. Bhardwaj A, Sapra L, Saini C, Azam Z, Mishra PK, Verma B, Mishra GC, Srivastava RK. COVID-19: immunology, immunopathogenesis and potential therapies. *Int Rev Immunol* 2022;41:171-206.  
[PUBMED](#) | [CROSSREF](#)
12. Papayannopoulos V. Neutrophil extracellular traps in immunity and disease. *Nat Rev Immunol* 2018;18:134-147.  
[PUBMED](#) | [CROSSREF](#)
13. Grilz E, Mauracher LM, Posch F, Königsbrügge O, Zöchbauer-Müller S, Marosi C, Lang I, Pabinger I, Ay C. Citrullinated histone H3, a biomarker for neutrophil extracellular trap formation, predicts the risk of mortality in patients with cancer. *Br J Haematol* 2019;186:311-320.  
[PUBMED](#) | [CROSSREF](#)
14. Kim SW, Lee H, Lee HK, Kim ID, Lee JK. Neutrophil extracellular trap induced by HMGB1 exacerbates damages in the ischemic brain. *Acta Neuropathol Commun* 2019;7:94.  
[PUBMED](#) | [CROSSREF](#)
15. Kaplan MJ, Radic M. Neutrophil extracellular traps: double-edged swords of innate immunity. *J Immunol* 2012;189:2689-2695.  
[PUBMED](#) | [CROSSREF](#)
16. Fuchs TA, Abed U, Goosmann C, Hurwitz R, Schulze I, Wahn V, Weinrauch Y, Brinkmann V, Zychlinsky A. Novel cell death program leads to neutrophil extracellular traps. *J Cell Biol* 2007;176:231-241.  
[PUBMED](#) | [CROSSREF](#)
17. Cedervall J, Zhang Y, Huang H, Zhang L, Femel J, Dimberg A, Olsson AK. Neutrophil extracellular traps accumulate in peripheral blood vessels and compromise organ function in tumor-bearing animals. *Cancer Res* 2015;75:2653-2662.  
[PUBMED](#) | [CROSSREF](#)

18. Katkar GD, Sundaram MS, NaveenKumar SK, Swethakumar B, Sharma RD, Paul M, Vishalakshi GJ, Devaraja S, Girish KS, Kemparaju K. NETosis and lack of DNase activity are key factors in *Echis carinatus* venom-induced tissue destruction. *Nat Commun* 2016;7:11361.  
[PUBMED](#) | [CROSSREF](#)
19. Cha MJ, Ha J, Lee H, Kwon I, Kim S, Kim YD, Nam HS, Lee HS, Song TJ, Choi HJ, et al. Neutrophil recruitment in arterial thrombus and characteristics of stroke patients with neutrophil-rich thrombus. *Yonsei Med J* 2022;63:1016-1026.  
[PUBMED](#) | [CROSSREF](#)
20. Inoue Y, Shirasuna K, Kimura H, Usui F, Kawashima A, Karasawa T, Tago K, Dezaki K, Nishimura S, Sagara J, et al. NLRP3 regulates neutrophil functions and contributes to hepatic ischemia-reperfusion injury independently of inflammasomes. *J Immunol* 2014;192:4342-4351.  
[PUBMED](#) | [CROSSREF](#)
21. Liu Z, Gao S, Bu Y, Zheng X. Luteolin protects cardiomyocytes cells against lipopolysaccharide-induced apoptosis and inflammatory damage by modulating Nlrp3. *Yonsei Med J* 2022;63:220-228.  
[PUBMED](#) | [CROSSREF](#)
22. Karmakar M, Katsnelson MA, Dubyak GR, Pearlman E. Neutrophil P2X7 receptors mediate NLRP3 inflammasome-dependent IL-1 $\beta$  secretion in response to ATP. *Nat Commun* 2016;7:10555.  
[PUBMED](#) | [CROSSREF](#)
23. O'Brien WT, Pham L, Symons GF, Monif M, Shultz SR, McDonald SJ. The NLRP3 inflammasome in traumatic brain injury: potential as a biomarker and therapeutic target. *J Neuroinflammation* 2020;17:104.  
[PUBMED](#) | [CROSSREF](#)
24. Liu D, Yang P, Gao M, Yu T, Shi Y, Zhang M, Yao M, Liu Y, Zhang X. NLRP3 activation induced by neutrophil extracellular traps sustains inflammatory response in the diabetic wound. *Clin Sci (Lond)* 2019;133:565-582.  
[PUBMED](#) | [CROSSREF](#)
25. Johnson JL, Ramadass M, Haimovich A, McGeough MD, Zhang J, Hoffman HM, Catz SD. Increased neutrophil secretion induced by *NLRP3* mutation links the inflammasome to azurophilic granule exocytosis. *Front Cell Infect Microbiol* 2017;7:507.  
[PUBMED](#) | [CROSSREF](#)
26. Skendros P, Papagoras C, Mitroulis I, Ritis K. Autoinflammation: lessons from the study of familial Mediterranean fever. *J Autoimmun* 2019;104:102305.  
[PUBMED](#) | [CROSSREF](#)
27. Stoler I, Freytag J, Orak B, Unterwalder N, Henning S, Heim K, von Bernuth H, Krüger R, Winkler S, Eschenhagen P, et al. Gene-dose effect of *MEFV* gain-of-function mutations determines *ex vivo* neutrophil activation in familial Mediterranean fever. *Front Immunol* 2020;11:716.  
[PUBMED](#) | [CROSSREF](#)
28. Mammana S, Fagone P, Cavalli E, Basile MS, Petralia MC, Nicoletti F, Bramanti P, Mazzon E. The role of macrophages in neuroinflammatory and neurodegenerative pathways of Alzheimer's disease, amyotrophic lateral sclerosis, and multiple sclerosis: pathogenetic cellular effectors and potential therapeutic targets. *Int J Mol Sci* 2018;19:831.  
[PUBMED](#) | [CROSSREF](#)
29. Perry VH, Cunningham C, Holmes C. Systemic infections and inflammation affect chronic neurodegeneration. *Nat Rev Immunol* 2007;7:161-167.  
[PUBMED](#) | [CROSSREF](#)
30. Wendeln AC, Degenhardt K, Kaurani L, Gertig M, Ulas T, Jain G, Wagner J, Häslers LM, Wild K, Skodras A, et al. Innate immune memory in the brain shapes neurological disease hallmarks. *Nature* 2018;556:332-338.  
[PUBMED](#) | [CROSSREF](#)
31. Jung H, Lee H, Kim D, Cheong E, Hyun YM, Yu JW, Um JW. Differential regional vulnerability of the brain to mild neuroinflammation induced by systemic LPS treatment in mice. *J Inflamm Res* 2022;15:3053-3063.  
[PUBMED](#) | [CROSSREF](#)
32. Hasenberg M, Köhler A, Bonifatius S, Borucki K, Riek-Burchardt M, Achilles J, Männ L, Baumgart K, Schraven B, Gunzer M. Rapid immunomagnetic negative enrichment of neutrophil granulocytes from murine bone marrow for functional studies *in vitro* and *in vivo*. *PLoS One* 2011;6:e17314.  
[PUBMED](#) | [CROSSREF](#)
33. Vaessen EM, Timmermans RA, Tempelaars MH, Schutyser MA, den Besten HM. Reversibility of membrane permeabilization upon pulsed electric field treatment in *Lactobacillus plantarum* WCFS1. *Sci Rep* 2019;9:19990.  
[PUBMED](#) | [CROSSREF](#)
34. Santoscoy MC, Jarboe LR. Streamlined assessment of membrane permeability and its application to membrane engineering of *Escherichia coli* for octanoic acid tolerance. *J Ind Microbiol Biotechnol* 2019;46:843-853.  
[PUBMED](#) | [CROSSREF](#)
35. Pérez-Peinado C, Dias SA, Domingues MM, Benfield AH, Freire JM, Rádis-Baptista G, Gaspar D, Castanho MA, Craik DJ, Henriques ST, et al. Mechanisms of bacterial membrane permeabilization by

- crotalicidin (Ctn) and its fragment Ctn(15-34), antimicrobial peptides from rattlesnake venom. *J Biol Chem* 2018;293:1536-1549.  
[PUBMED](#) | [CROSSREF](#)
36. Leong SY, Ong BK, Chu JJ. The role of Misshapen NCK-related kinase (MINK), a novel Ste20 family kinase, in the IRES-mediated protein translation of human enterovirus 71. *PLoS Pathog* 2015;11:e1004686.  
[PUBMED](#) | [CROSSREF](#)
  37. Pino PA, Cardona AE. Isolation of brain and spinal cord mononuclear cells using percoll gradients. *J Vis Exp* 2011:2348.  
[PUBMED](#) | [CROSSREF](#)
  38. Watson PM, Anderson JM, VanTallie CM, Doctrow SR. The tight-junction-specific protein ZO-1 is a component of the human and rat blood-brain barriers. *Neurosci Lett* 1991;129:6-10.  
[PUBMED](#) | [CROSSREF](#)
  39. Sulowska Z, Majewska E, Klink M, Banasik M, Tchórzewski H. Flow cytometric evaluation of human neutrophil apoptosis during nitric oxide generation *in vitro*: the role of exogenous antioxidants. *Mediators Inflamm* 2005;2005:81-87.  
[PUBMED](#) | [CROSSREF](#)
  40. Tsao FH, Xiang Z, Abbasi A, Meyer KC. Neutrophil necrosis and annexin 1 degradation associated with airway inflammation in lung transplant recipients with cystic fibrosis. *BMC Pulm Med* 2012;12:44.  
[PUBMED](#) | [CROSSREF](#)
  41. Holtmaat A, Bonhoeffer T, Chow DK, Chuckowree J, De Paola V, Hofer SB, Hübener M, Keck T, Knott G, Lee WC, et al. Long-term, high-resolution imaging in the mouse neocortex through a chronic cranial window. *Nat Protoc* 2009;4:1128-1144.  
[PUBMED](#) | [CROSSREF](#)
  42. Byun DJ, Kim YM, Hyun YM. Real-time observation of neutrophil extracellular trap formation in the inflamed mouse brain via two-photon intravital imaging. *Lab Anim Res* 2022;38:16.  
[PUBMED](#) | [CROSSREF](#)
  43. Reber LL, Gillis CM, Starkl P, Jönsson F, Sibilano R, Marichal T, Gaudenzio N, Bérard M, Rogalla S, Contag CH, et al. Neutrophil myeloperoxidase diminishes the toxic effects and mortality induced by lipopolysaccharide. *J Exp Med* 2017;214:1249-1258.  
[PUBMED](#) | [CROSSREF](#)
  44. Jaw JE, Tsuruta M, Oh Y, Schipilow J, Hirano Y, Ngan DA, Suda K, Li Y, Oh JY, Moritani K, et al. Lung exposure to lipopolysaccharide causes atherosclerotic plaque destabilisation. *Eur Respir J* 2016;48:205-215.  
[PUBMED](#) | [CROSSREF](#)
  45. Sarsenbaeva AS, Ivanova EL, Burmistrova AL, Drozdov IV. The character of the morphological changes of the mucous membrane of the large intestine and the genetic polymorphism of IL-1RA, IL-1B, IL-4 TNFA in patient with irritable bowel syndrome. *Eksp Klin Gastroenterol* 2013:28-33.  
[PUBMED](#)
  46. Hoppenbrouwers T, Autar AS, Sultan AR, Abraham TE, van Cappellen WA, Houtsmuller AB, van Wamel WJ, van Beusekom HM, van Neck JW, de Maat MP. *In vitro* induction of NETosis: comprehensive live imaging comparison and systematic review. *PLoS One* 2017;12:e0176472.  
[PUBMED](#) | [CROSSREF](#)
  47. Li RH, Ng G, Tablin F. Lipopolysaccharide-induced neutrophil extracellular trap formation in canine neutrophils is dependent on histone H3 citrullination by peptidylarginine deiminase. *Vet Immunol Immunopathol* 2017;193-194:29-37.  
[PUBMED](#) | [CROSSREF](#)
  48. Pieterse E, Rother N, Yanginlar C, Hilbrands LB, van der Vlag J. Neutrophils discriminate between lipopolysaccharides of different bacterial sources and selectively release neutrophil extracellular traps. *Front Immunol* 2016;7:484.  
[PUBMED](#) | [CROSSREF](#)
  49. Kuczia P, Zuk J, Iwaniec T, Soja J, Dropinski J, Malesa-Wlodzik M, Zareba L, Bazan JG, Undas A, Bazan-Socha S. Citrullinated histone H3, a marker of extracellular trap formation, is increased in blood of stable asthma patients. *Clin Transl Allergy* 2020;10:31.  
[PUBMED](#) | [CROSSREF](#)
  50. Thålin C, Lundström S, Seignez C, Daleskog M, Lundström A, Henriksson P, Helleday T, Phillipson M, Wallén H, Demers M. Citrullinated histone H3 as a novel prognostic blood marker in patients with advanced cancer. *PLoS One* 2018;13:e0191231.  
[PUBMED](#) | [CROSSREF](#)
  51. Rummel C, Inoue W, Poole S, Luheshi GN. Leptin regulates leukocyte recruitment into the brain following systemic LPS-induced inflammation. *Mol Psychiatry* 2010;15:523-534.  
[PUBMED](#) | [CROSSREF](#)

52. Kim YR, Kim YM, Lee J, Park J, Lee JE, Hyun YM. Neutrophils return to bloodstream through the brain blood vessel after crosstalk with microglia during LPS-induced neuroinflammation. *Front Cell Dev Biol* 2020;8:613733.  
[PUBMED](#) | [CROSSREF](#)
53. Ode Y, Aziz M, Jin H, Arif A, Nicastro JG, Wang P. Cold-inducible rna-binding protein induces neutrophil extracellular traps in the lungs during sepsis. *Sci Rep* 2019;9:6252.  
[PUBMED](#) | [CROSSREF](#)
54. Perdomo J, Leung HH, Ahmadi Z, Yan F, Chong JJ, Passam FH, Chong BH. Neutrophil activation and NETosis are the major drivers of thrombosis in heparin-induced thrombocytopenia. *Nat Commun* 2019;10:1322.  
[PUBMED](#) | [CROSSREF](#)
55. Fatemi A, Alipour R, Khanahmad H, Alsahebfofusol F, Andalib A, Pourazar A. The impact of neutrophil extracellular trap from patients with systemic lupus erythematosus on the viability, CD11b expression and oxidative burst of healthy neutrophils. *BMC Immunol* 2021;22:12.  
[PUBMED](#) | [CROSSREF](#)
56. McDonald B, Urrutia R, Yipp BG, Jenne CN, Kubes P. Intravascular neutrophil extracellular traps capture bacteria from the bloodstream during sepsis. *Cell Host Microbe* 2012;12:324-333.  
[PUBMED](#) | [CROSSREF](#)
57. Kolaczowska E, Jenne CN, Surewaard BG, Thanabalasuriar A, Lee WY, Sanz MJ, Mowen K, Opendakker G, Kubes P. Molecular mechanisms of NET formation and degradation revealed by intravital imaging in the liver vasculature. *Nat Commun* 2015;6:6673.  
[PUBMED](#) | [CROSSREF](#)
58. Cichon I, Ortmann W, Santocki M, Opydo-Chanek M, Kolaczowska E. Scrutinizing mechanisms of the 'obesity paradox in sepsis': Obesity is accompanied by diminished formation of neutrophil extracellular traps (nets) due to restricted neutrophil-platelet interactions. *Cells* 2021;10:384.  
[PUBMED](#) | [CROSSREF](#)
59. Cools-Lartigue J, Spicer J, McDonald B, Gowing S, Chow S, Giannias B, Bourdeau F, Kubes P, Ferri L. Neutrophil extracellular traps sequester circulating tumor cells and promote metastasis. *J Clin Invest* 2013;123:3446-3458.  
[PUBMED](#) | [CROSSREF](#)
60. Lochhead JJ, Yang J, Ronaldson PT, Davis TP. Structure, function, and regulation of the blood-brain barrier tight junction in central nervous system disorders. *Front Physiol* 2020;11:914.  
[PUBMED](#) | [CROSSREF](#)
61. Wang Y, Peng F, Xie G, Chen ZQ, Li HG, Tang T, Luo JK. Rhubarb attenuates blood-brain barrier disruption via increased zonula occludens-1 expression in a rat model of intracerebral hemorrhage. *Exp Ther Med* 2016;12:250-256.  
[PUBMED](#) | [CROSSREF](#)
62. Mizee MR, Wooldrik D, Lakeman KA, van het Hof B, Drexhage JA, Geerts D, Bugiani M, Aronica E, Mebius RE, Prat A, et al. Retinoic acid induces blood-brain barrier development. *J Neurosci* 2013;33:1660-1671.  
[PUBMED](#) | [CROSSREF](#)
63. Tall AR, Westerterp M. Inflammasomes, neutrophil extracellular traps, and cholesterol. *J Lipid Res* 2019;60:721-727.  
[PUBMED](#) | [CROSSREF](#)
64. Denes A, Pinteaux E, Rothwell NJ, Allan SM. Interleukin-1 and stroke: biomarker, harbinger of damage, and therapeutic target. *Cerebrovasc Dis* 2011;32:517-527.  
[PUBMED](#) | [CROSSREF](#)
65. Mendiola AS, Cardona AE. The IL-1 $\beta$  phenomena in neuroinflammatory diseases. *J Neural Transm (Vienna)* 2018;125:781-795.  
[PUBMED](#) | [CROSSREF](#)
66. Simi A, Tsakiri N, Wang P, Rothwell NJ. Interleukin-1 and inflammatory neurodegeneration. *Biochem Soc Trans* 2007;35:1122-1126.  
[PUBMED](#) | [CROSSREF](#)
67. Rumble JM, Huber AK, Krishnamoorthy G, Srinivasan A, Giles DA, Zhang X, Wang L, Segal BM. Neutrophil-related factors as biomarkers in EAE and MS. *J Exp Med* 2015;212:23-35.  
[PUBMED](#) | [CROSSREF](#)
68. Aubé B, Lévesque SA, Paré A, Chamma É, Kébir H, Gorina R, Lécuyer MA, Alvarez JI, De Koninck Y, Engelhardt B, et al. Neutrophils mediate blood-spinal cord barrier disruption in demyelinating neuroinflammatory diseases. *J Immunol* 2014;193:2438-2454.  
[PUBMED](#) | [CROSSREF](#)
69. Gimenez F, Bhela S, Dogra P, Harvey L, Varanasi SK, Jaggi U, Rouse BT. The inflammasome NLRP3 plays a protective role against a viral immunopathological lesion. *J Leukoc Biol* 2016;99:647-657.  
[PUBMED](#) | [CROSSREF](#)